Analytic design of hybrid diffractive–refractive achromats

N. Davidson, A. A. Friesem, and E. Hasman

An analytic design of hybrid achromats that combine refractive and diffractive elements is presented. The design procedure does not rely on paraxial approximations and involves two separate stages. In the first stage the chromatic aberrations are corrected for the paraxial rays, and in the second stage the spherical aberrations are corrected by addition of an aspherical phase function to the diffractive element. The residual spherochromatic aberrations of the achromat are evaluated both analytically and numerically, with good agreement between the results. Finally, we illustrate the design procedure by designing a plano–convex achromat for IR radiation with little chromatic dispersion.

1. Introduction

Diffractive and refractive elements can be combined to eliminate, or at least significantly reduce, chromatic aberrations.[1–4] These so-called hybrid achromats exploit the fact that the dispersion of refractive elements is opposite that of diffractive elements,[1] so they can cancel each other. The attractive aspect of hybrid achromats is that, unlike wholly refractive achromats, they require only one type of refracting material, and the curvatures of the refractive surfaces are not as extreme.

The usual approaches to designing hybrid achromats involve numerical techniques that are based on established design routines for refractive elements.[3] The more general analytic design approaches have thus far included paraxial approximations, so they were confined to elements with relatively large f numbers.[2] In this paper we introduce an analytic design of hybrid achromats that does not rely on paraxial approximations, although thin-lens approximations are still used to simplify the mathematical treatment. Our approach is thus applicable to elements with relatively low f numbers. It can yield more general solutions as well as better physical insight than the numerical optimization techniques. To illustrate our approach, we designed a hybrid focusing lens for IR radiation. The performance of the lens is analyzed by ray tracing, and the results are compared with those of a standard singlet. Finally, we discuss how to generalize our approach to include the finite thickness of the elements, so as to extend its validity to elements with even smaller f numbers.

2. Achromat Design Procedure

In general, the goals for a proper design of achromats are to minimize both chromatic and spherical aberrations. These are also the goals in our approach to designing a hybrid achromat of the form shown in Fig. 1; as shown, the achromat comprises a refractive element and an adjacent diffractive element.

With our approach, one can correct the first-order chromatic aberrations first by properly dividing the paraxial optical power (the inverse of the focal distance) between the diffractive element and the refractive element.[2] Then the spherical aberrations of the refractive lens are calculated with a thin-lens approximation,[5] and they are corrected by incorporation of the opposite aberrations into the diffractive surface. Finally, the residual aberrations, known as spherochromatism,[5] are evaluated to ensure that they are not excessive.

A. Chromatic Aberrations

The chromatic dispersion of a refractive element is usually characterized by its Abbé V number,[2] which is defined as

$$V_r = \frac{n_d - 1}{n_f - n_c}, \tag{1}$$

When this research was done the authors were with the Department of Electronics, Weizmann Institute of Science, Rehovot 76100, Israel. N. Davidson is now with the Department of Physics, Stanford University, Stanford, California 94305. A. A. Friesem is also with the Heinrich Herz Institute, Berlin 10, Germany. E. Hasman is now with Optrotech Ltd., P.O.B. 69, Nes Ziona 70450, Israel.

Received 4 August 1992.
0003-6935/93/254770-05$06.00/0.

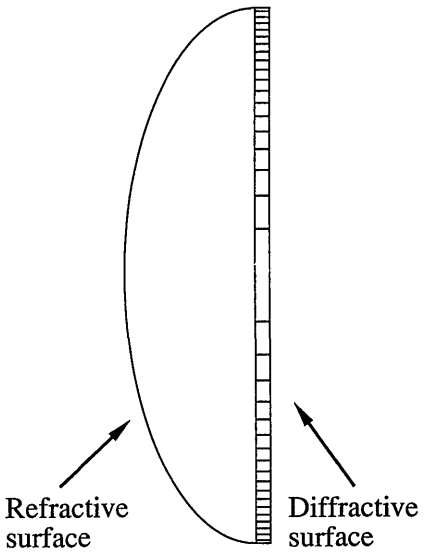

Fig. 1. Schematic representation of a hybrid diffractive–refractive achromat.

where n_c, n_d, and n_f are the refractive indices at wavelengths λ_c, λ_d, and λ_f, respectively. The three wavelengths usually denote three standard lines in some spectral range. For example, in the visible regime λ_c, λ_d, and λ_f are the classical spectroscopic wavelengths of 0.6563, 0.5876, and 0.4861 μm, respectively. In the IR regime λ_c, λ_d, and λ_f could be 12, 10, and 8 μm, respectively. It is also possible to characterize the chromatic dispersion of a diffractive element in a similar manner, where the diffractive V number is defined as[2]

$$V_d = \frac{\lambda_d}{\lambda_f - \lambda_c}. \tag{2}$$

Note that the V number for diffactive elements is negative (assuming $\lambda_f < \lambda_c$), whereas the V number for refractive elements is always positive. Therefore, by properly dividing the paraxial optical power, which is related directly to the V numbers, between the refractive and diffractive elements, it is possible to reduce the overall chromatic dispersions of hybrid elements. Assuming negligible separation between the refractive and diffractive elements, this optical division of the paraxial optical power is[2]

$$f_{d,0} = F\left(\frac{V_d - V_r}{V_d}\right), \qquad f_{r,0} = F\left(\frac{V_r - V_d}{V_r}\right). \tag{3}$$

where $f_{d,0}$ and $f_{r,0}$ are the paraxial focal distances of the diffractive and refractive elements, respectively, and F is the desired focal distance of the hybrid element.

B. Spherical Aberrations

Consider a thin refractive lens in air with paraxial focal distance $f_{r,0}$, refractive index n, and radii of curvature r_1 and r_2 for the front and rear surfaces, respectively. This lens contributes the following amount to the primary spherical aberrations at the final image[5]:

$$S = -y^2 f_{r,0}^2 (G_1 c^3 - G_2 c^2 c_1 + G_3 c^2 v_1 + G_4 c c_1^2 - G_5 c c_1 v_1 + G_6 c v_1^2), \tag{4}$$

where y is the distance from the optical axis, v_1 is the reciprocal of the object distance to the element, $c_1 = 1/r_1$, $c = 1/f(n-1)$, and the G terms are complicated functions of the refractive index of the lens.[5] When we assume an incoming plane wave ($v_1 = 0$) and a plano–convex lens ($c_1 = c$), Eq. (4) simplifies to

$$S = \frac{y^2}{(n-1)^3 f_{r,0}} (G_1 - G_2 + G_4), \tag{5}$$

with

$$G_1 = \tfrac{1}{2} n^2 (n-1),$$

$$G_2 = \tfrac{1}{2}(2n+1)(n-1),$$

$$G_4 = \tfrac{1}{2}(n+2)(n-1)/n.$$

The alternative choice for a plano–convex lens ($c_1 = 0$) would yield spherical aberrations with approximately double magnitude.[5] Equation (5) indicates that an incoming ray, parallel at a distance y to the optical axis, will be focused to a distance $f_r(y)$ from the lens along the optical axis, given as[5]

$$f_r(y) \approx f_{r,0} + a y^2, \tag{6}$$

where

$$a = (G_1 - G_2 + G_4)/f_{r,0}(n-1)^3,$$

and higher-order terms in y are neglected.

Now the desired focal distance for the diffractive surface $f_d(y)$ should be such that the focal distance F (independent of y) at the central wavelength λ_d for the combination of diffractive and refractive elements is a constant. Assuming negligible separation between the refractive and diffractive elements, we resort to a simple lens combination equation:

$$\frac{1}{f_r(y)} + \frac{1}{f_d(y)} = \frac{1}{F} = \text{const.}, \tag{7}$$

where F is the desired focal distance of the hybrid lens. Solving Eq. (7) for $f_d(y)$ yields

$$f_d(y) = \frac{f_r(y) F}{f_r(y) - F}. \tag{8}$$

Finally, to find the phase function for the diffractive element $\phi(y)$ that would provide a focal distance $f_d(y)$, we resort to the diffraction relation[6]

$$\frac{d\phi(y)}{dy} = \frac{2\pi}{\lambda_d} \frac{-y}{[y^2 + f_d^2(y)]^{1/2}}. \tag{9}$$

In the general case, one can find $\phi(y)$ by integrating Eq. (9) numerically. However, in some cases $f_d(y)$ may be expanded as a power series in the small parameter $ay^2/f_{r,0}$, and retaining only the first two terms, we have

$$f_d(y) \approx f_{d,0} + a'y^2, \tag{10}$$

where

$$a' = -a(f_{d,0}/f_{r,0})^2.$$

When such an expansion is valid, Eq. (9) can be integrated analytically to yield

$$\phi(y) = \frac{-2\pi}{\lambda_d a'} \ln\{2a'[a'^2y^4 + (2f_{d,0}a' + 1)y^2 + f_{d,0}^2]^{1/2} + 2a'^2y^2 + 2a'f_{d,0} + 1\}. \tag{11}$$

C. Spherochromatism

So far we have dealt with the chromatic aberrations and the spherical aberrations separately. Specifically we corrected the chromatic aberrations for the paraxial rays only and corrected the spherical aberrations for the central wavelength λ_d only. Thus, for nonparaxial rays that are also with wavelengths different from λ_d , we may expect to find residual aberrations known as spherochromatism.[5]

To estimate these residual aberrations for the marginal rays M (where they are expected to be maximal[5]), we regard the aspheric component of $\phi(y)$ as the phase function for another diffractive element that is added to the paraxial (spherical) hybrid achromat. This addition component is chosen so as to cancel the spherical aberrations S at λ_d and will lead to a separate focal distance at this wavelength $f_{\text{additional}}(M, \lambda_d)$ that obeys the approximation

$$\frac{1}{f_{\text{additional}}(M, \lambda_d)} \approx \frac{1}{F} - \frac{1}{F + S}. \tag{12}$$

In general, at any other wavelength λ, this additional focal distance is

$$f_{\text{additional}}(M, \lambda) = f_{\text{additional}}(M, \lambda_d)\lambda_d/\lambda. \tag{13}$$

If we neglect the wavelength dependence of S for the paraxial hybrid achromat (this is justified in the next section by the result in Fig. 3), we can approximate the (marginal) focal distance of the aspheric hybrid achromat at any wavelength $f_{\text{aspheric}}(M, \lambda)$ by

$$\frac{1}{f_{\text{aspheric}}(M, \lambda)} \approx \frac{1}{f_{\text{spheric}}(M)} + \frac{1}{f_{\text{additional}}(M, \lambda)}. \tag{14}$$

When we combine Eqs. (12), (13), and (14) and assume that S is much smaller than F, the residual spherochromatic aberrations for the marginal rays are

$$f_{\text{aspheric}}(M, \lambda_c) - f_{\text{aspheric}}(M, \lambda_f) \approx S\delta\lambda/\lambda_d, \tag{15}$$

where $\delta\lambda = \lambda_c - \lambda_f$ represents the entire relevant spectral range and $\lambda_c\lambda_f \approx \lambda_d^2$ is assumed. Relation (15) can be intuitively explained by the following reasoning: the aspheric component of $\phi(y)$, which is perfectly suited to correcting the spherical aberrations S for the central wavelength, has itself a relative error of $\delta\lambda/\lambda_d$ over the entire spectral range. However, since the focal distances of lenses that are combined do not simply add up, a formal rather than intuitive derivation of relation (15) is needed.

Relation (15) is by no means a lower limit to the amount of the residual spherochromatic aberrations of any hybrid achromat. It applies only to the specific design procedure that is described above. Nevertheless it does point out a general trend in hybrid achromats in which the spherical aberrations of spherical refractive surfaces are corrected by an aspherical phase function of a diffractive element—the introduction of significant spherochromatic aberrations as given in relation (15). For comparison, if the spherical aberrations are corrected with an aspherical refractive element, whereas the diffractive element corrects only the chromatic aberrations, no first-order spherochromatic aberrations are expected.

3. Illustrative Example for a Singlet Design

We illustrate our design approach with a specific example of transforming a plano–convex gallium arsenide (GaAs) focusing singlet to an achromat. We consider a commercially available lens with a diameter of 25.4 mm ($y_{\max}$ = 12.7 mm), a focal distance of 76.2 mm (f number = 3.0), and a maximal thickness of 2 mm. Such GaAs lenses are mainly used for thermal imaging; so we chose the c, d, and f wavelengths to be 12, 10, and 8 μm, respectively, resulting in $V_d = -2.5$ according to Eq. (2). The refractive index of GaAs at these wavelengths[7] is 3.262, 3.270, and 3.284, respectively, resulting in $V_r = 103.2$, according to Eq. (1). The optical performance of this singlet was calculated with the aid of a ray-tracing computer design program that can handle both spherical refractive surfaces and general aspheric diffractive phase functions. The results presented in Fig. 2 depict the variation of the focal distance as a function of the distance of the incoming ray from the optical axis of the lens for the wavelengths of 8, 10, and 12 μm; these results reveal that the maximal chromatic aberrations of the singlet are 0.75 mm, and the maximal spherical aberrations (for the marginal rays) are 0.95 mm, so the maximal total aberrations are 1.7 mm. For comparison the diffraction-limited focal depth of the singlet is only $2.5\lambda f_{\#}^2 \approx 0.2$ mm. The results of the numerically calculated spherical aberrations shown in Fig. 2 agree with those predicted by Eq. (6) within 0.005 mm for any radius; this confirms the validity of Eq. (6) and the approximation that was used to obtain it.

The first stage of our design involves the correction of the paraxial chromatic aberrations by adding a diffractive element with a spherical phase function to yield a simplified (paraxial) hybrid achromat. The

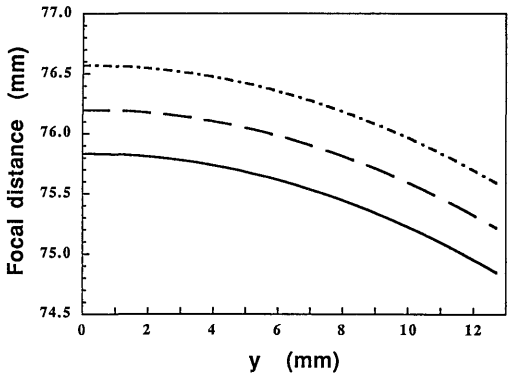

Fig. 2. Variation of the focal distance as a function of the distance of the incoming ray from the optical axis of the GaAs singlet at wavelengths of 8 μm (solid curve), 10 μm (dashed curve), and 12 μm (dashed–dotted curve).

paraxial focal distances of the diffractive and refractive elements that minimize the chromatic aberrations are found from Eq. (3) to be $f_{r,0} = 78$ mm and $f_{d,0} = 3222$ mm. Figure 3 shows the variation in the focal distance as a function of y at the central wavelength of 10 μm for this spherical achromat. The corresponding results for the wavelengths of 8 and 12 μm deviate by < 0.025 mm for all y terms and would not be distinguishable from the curve in Fig. 3; this indicates that the spherical aberrations are indeed independent of wavelength at this stage, as was assumed above when we estimated the residual spherochromatism. Moreover these results indicate that the maximal chromatic aberrations for the paraxial achromat have been reduced by a factor of 300. However, the spherical aberrations at the maximal radius are still 0.95 mm, the same as for the GaAs singlet; this is expected since the spherical phase function of the diffractive element contributes no spherical aberrations.[8]

To reduce the spherical aberrations of the hybrid achromat, the spherical phase function of the diffractive element is now replaced with an aspheric phase function, which is obtained by numerical integration of Eq. (9). In this case the expansion parameter of Eq. (10) is no longer small, so the analytic expression for $\phi(y)$ in Eq. (11) is not valid. The optical performance of this aspheric hybrid achromat is calculated as before, and the results are presented in Fig. 4. They show the variation of the focal distance as a function of the distance of the incoming ray from the axis of the lens for the wavelengths of 8, 10, and 12 μm. Several interesting features emerge from Fig. 4. First, the paraxial chromatic aberrations (i.e., the difference in the focal distance between the three wavelengths near the optical axis) are very small (< 0.01 mm). Second, the spherical aberrations for the central wavelength (for which the aspheric phase was designed) are also relatively small (< 0.025 mm). Finally, the residual spherochromatic aberrations (that refer to rays with wavelengths that are different from the central wavelength, which are also far from the optical axis) are 0.40 mm, in excellent agreement with the value of 0.38 mm, as predicted by relation (15). This indicates that the finite thickness of the hybrid element (2 mm) as well as higher-order spherical aberrations have little effect on the optical performance.

It is possible to reduce the spherochromatic aberrations by a factor of ~ 2 if the chromatic aberrations were corrected for the zonal rays[5] rather than the paraxial ones. This complicates somewhat the design procedure, since the two design stages (chromatic aberration correction and spherical aberration correction) are no longer independent, and several iterations between them must be performed. The result from such an improved design procedure is shown in Fig. 5. The residual spherochromatic aberrations here are now ~ 0.22 mm, which is indeed half of those obtained with the original procedure (Fig. 4) and ~ 8 times smaller than the total aberrations of the GaAs singlet; in fact, they are of the same order as the diffraction-limited focal depth.

4. Concluding Remarks

We have presented a general analytic design for hybrid achromats that combines reflective and diffractive elements. The design does not rely on paraxial approximations and involves two separate stages.

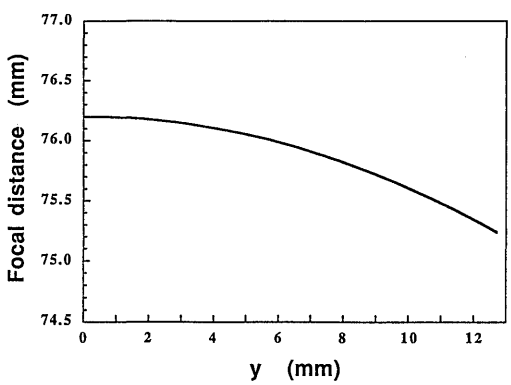

Fig. 3. Variation of the focal distance as a function of the distance of the incoming ray from the optical axis of the simple paraxial (spherical) hybrid achromat at a 10-μm wavelength.

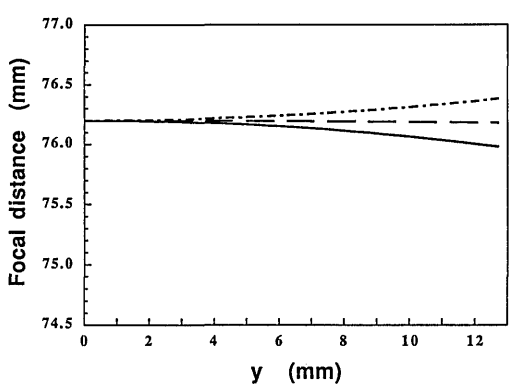

Fig. 4. Variation of the focal distance as a function of distance of the incoming ray from the optical axis of the aspheric hybrid achromat at wavelengths of 8 μm (solid curve), 10 μm (dashed line), and 12 μm (dashed–dotted curve).

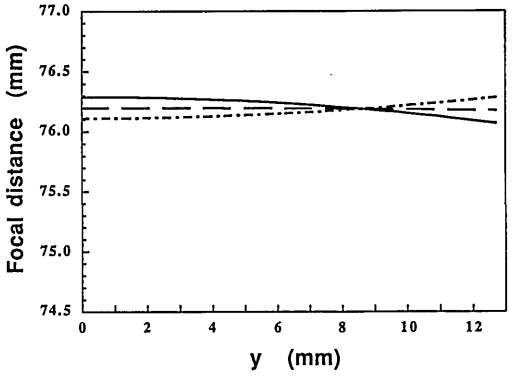

Fig. 5. Variation of the focal distance as a function of the distance of the incoming ray from the optical axis of the improved aspheric hybrid achromat (chromatic aberrations corrected for the zonal ray) at wavelengths of 8 μm (solid curve), 10 μm (dashed line) and 12 μm (dashed–dotted curve).

In the first stage the chromatic aberrations are corrected for the paraxial rays, and in the second stage the spherical aberrations are corrected by addition of an aspherical phase function to the diffractive element. The residual spherochromatic aberrations of the achromat were evaluated both analytically and numerically, with good agreement between the results. It was shown that such residual aberrations are proportional to the original spherical aberrations of the lens and to the spectral bandwidth of the illumination.

In this paper we concentrated on plano–convex lenses for the IR wavelength regime. Such lenses are particularly advantageous because they are relatively simple, and the diffractive element can be recorded directly on the planar surface with standard photolithographic techniques.[9] Nevertheless our design approach can be readily applied also to more general lenses, where the diffractive element can be formed on a curved surface, for example, with diamond-turning techniques; such hybrid achromats may have lower aberrations than the plano–convex achromats presented here because of the additional degree of freedom that is available.

It is also possible to include in our analytical design the finite thickness of the refractive lens and a possible separation between the refractive lens and the diffractive surface. We can do this by replacing Eq. (4) by the exact contributions to the spherical aberration of each refracting surface,[5] and by applying the exact total contribution at the plane of the diffractive element instead of using the thin-lens combination of Eq. (7). The resulting expression for $f_d(y)$ would still be analytical (although more complicated), but to find the phase function of the diffractive element one should integrate Eq. (9) numerically. We checked the affects of such thick-lens corrections for the specific hybrid achromat presented in Section 3 (GaAs, $f/3$) and found them to be negligible; nevertheless for smaller f numbers (and therefore larger thicknesses) these corrections become more important.

Finally, although our design does not necessarily provide the optimal achromat, it can give approximate solutions or serve as a starting point for a more comprehensive optimization with iterative ray-tracing computer programs.

References

1. R. H. Katyal, "Compensating optical systems. Parts 1–3," Appl. Opt. **11,** 1241–1260 (1972).
2. T. Stone and N. George, "Hybrid diffractive–refractive lenses and achromats," Appl. Opt. **27,** 2960–2971 (1988).
3. G. J. Swanson and W. B. Veldkamp, "Diffractive optical elements for use in infrared systems," Opt. Eng. **28,** 605–608 (1989).
4. K. E. Spaulding and G. M. Morris, "Achromatic waveguide lenses," Appl. Opt. **30,** 2558–2569 (1991).
5. R. Kingslate, *Lens Design Fundamentals* (Academic, New York, 1978), p. 115.
6. L. B. Felsen, "Real spectra, complex spectra, compact spectra," J. Opt. Soc. Am. A **3,** 486–496 (1986).
7. A. R. Peaker, *Properties of Galluim Arsenide* (Institute of Electrical Engineers, London, 1990), p. 250.
8. D. H. Close, "Holographic optical elements," Opt. Eng. **14,** 408–413 (1975).
9. E. Hasman, N. Davidson, and A. A. Friesem, "Efficient multilevel phase holograms for CO_2 lasers," Opt. Lett. **16,** 423–425 (1991).